

# ROBUST DTC OF AN ADJUSTABLE SPEED SENSORLESS SWITCHED RELUCTANCE MOTORS BASED ON SVM USING A PI PREDICTIVE CONTROLLER

**M. BIRAME    L.MOKRANI**

Materials Laboratory, Electrical Engineering Department, Laghouat University, BP 37G, Ghardaia Street, Laghouat (03000), Algeria, E-mail : bir\_moh@yahoo.fr, Mokrani\_lakhdar@hotmail.com

**B. AZOUI**

LEB Laboratory, Electrical Engineering Department, Batna University, Chahid M.E.H. Boukhlof Street, Batna (05000), Algeria, Azoui\_b@yahoo.com

**A. Naamane N.K. Msird**

LSIS - Laboratory of the System and Information sciences, marseille, Paul Czanne University , FRANCE  
aziz.naamane@lsis.org, nacer.msirdi@lsis.org

*Abstract: In This study presents a new sensorless direct torque control method for voltage inverter fed RSM. The control method is used a modified Direct Torque Control scheme with constant inverter switching frequency using Space Vector Modulation (SVPWM). The variation of stator resistance due to changes in temperature or frequency deteriorates the performance of DTC-SVM controller by introducing errors in the estimated flux linkage and the electromagnetic torque. As a result, this approach will not be suitable for high power drives such as those used in tractions, as they require good torque control performance at considerably lower frequency. A novel stator resistance estimator is proposed. The estimation method is implemented using the Extended Kalman Filter. Finally, extensive simulation results are presented to validate the proposed technique. The system is tested to change in value of the stator resistance and a very satisfactory efficiency was obtained..*

**Key words:** RSM, DTC-SVPWM, observerless and sensorless speed control, Extended Kalman Filter (EKF).DTC, SVM,.

## 1. Introduction.

Reluctance Synchronous Motors (RSM) has attracted significant interest of industry due to their main advantages are [1-3]:

- Simplicity and robustness
- High torque overloads capacity
- High efficiency over wide speed-range
- Low machine inertia
- decreased maintenance requirements

The absence of windings and magnets on the rotor enables SR motors to run high speed and temperature. An SR motor can produce large torque in a wide speed range. However, it has some drawbacks such as torque ripple and acoustic noise. High torque ripple is

inevitable unless ripple reduction strategy is applied. Firstly DTC was proposed for IM [3], however now is applied also for PMSM and RSM[4]. Direct Torque Control (DTC) seems to be a good performance alternative to the classical vector control drives. After its implementation on induction motor drives, this control method in recent years has been proposed for synchronous reluctance motor with good results. DTC is able to produce fast torque and stator flux response with a well designed flux, torque and speed estimator. In order to reduce the torque and current pulsations, in steady state a mixed DTC- SVM control method seems more suitable [1, 6].

SVM techniques [5 6] offer better DC link utilization and they lower the torque ripple. The emphasis of research on RSM has been on sensorless drive [7, 8, 9, 10], which eliminates flux and speed sensors mounted on the motor. In addition, the development of effective speed and flux estimators has allowed good rotor flux-oriented performance at all speeds except those close to zero. Sensorless control has improved the motor performance, compared to the Volts/Hertz (or constant flux) controls.

The EKF is considered to be suitable for use in high-performance RSM drives, and it can provide accurate speed estimates in a wide speed-range, including very low speed [5] [10, 11].

The variation of stator resistance due to changes in temperature or frequency deteriorates the performance of DTC controller by introducing errors in the estimated flux linkage and the electromagnetic torque [13-16]. A novel stator resistance estimator during the operation of the motor is proposed.

This paper describes a novel DTC-SVM method for a speed sensorless control of RSM drive. According to this method, a conventional PI predictive controller is used to determine the polar components of the voltage command vector. The results show that a satisfactory control performance is obtained.

## 2. Modeling of the RSM.

The electrical and mechanical equations of the RSM in the rotor reference (d,q) frame as follows

$$\begin{cases} \frac{dI_d}{dt} = -\frac{R_s}{L_d} + \frac{L_q}{L_d} P \hat{S}_r I_q + \frac{1}{L_d} U_d \\ \frac{dI_q}{dt} = -\frac{R_s}{L_q} - \frac{L_d}{L_q} P \hat{S}_r I_d + \frac{1}{L_q} U_q \\ \frac{d\hat{S}_r}{dt} = \frac{3P}{2J} (L_d - L_q) I_d I_q - \frac{1}{J} T_L - \frac{B}{J} \hat{S}_r \end{cases} \quad (1)$$

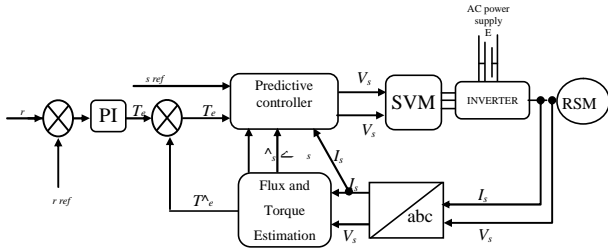


Fig. 1. RSM Drive System Control.

where  $I_d, I_q$  are the d-q axis currents,  $U_d, U_q$  are the d-q axis voltages,  $\omega$  denotes the rotor speed,  $R_s$  is the stator resistance,  $L_d, L_q$  are the stator inductances,  $P$  is the pole pairs,  $J$  is the rotor moment of inertia,  $B$  is the viscous friction coefficient,  $T_L$  is the load torque.

The block scheme of the investigated direct torque control with space vector modulation (DTC-SVM) for a voltage source PWM inverter fed RSM is presented in Fig 1(a). [5, 6]

The internal structure of the predictive torque and flux controller is shown in Fig 1(b).

The objective of the DTC-SVM scheme, and the main difference between the classic DTC, is to estimate a reference stator voltage vector  $V_{sref}$  in order to drive the power gates of the inverter with a constant switching frequency. Although, the basic principle of the DTC is that the electromagnetic torque of the motor can be adjusted by controlling the angle  $\alpha$  between the stator and rotor flux vectors, the torque of a RSM can be calculated by the following equation [5, 6]

$$T_e = \frac{3}{2} P \frac{\Phi_{s-ref}}{L_d L_q} \left( \frac{1}{2} \Phi_{s-ref} (L_d - L_q) \sin 2\alpha \right) \quad (2)$$

Where the change in the stator flux vector, if we neglect the voltage drop in the stator resistance, can be given by the following equation,

$$\Delta \Phi_s = V_s T_s \quad (3)$$

Where  $\Delta$  is the deviation from  $|\Phi_s|$  which are

defined by:

$$\Delta \Phi_s = |\Phi_{sref}| - |\Phi_s| \quad (4)$$

The predictive controller determinates the stator voltage command vector in polar coordinates  $V_{sref}$  [5, 6] for space vector modulator; which finally generates the pulses  $S_a, S_b, S_c$ .

Sampled torque error  $T_e$  and reference stator flux amplitude  $\Phi_{sref}$  are delivered to the predictive controller. The relation between error of torque and increment of load and angle is nonlinear. Therefore PI controller, which generates the load angle increment required to minimize the instantaneous error between reference  $T_{eref}$  and actual  $T_e$  torque, has been applied. The reference values of the stator voltage  $V_{sref}$ ,  $\Phi_{sref}$  is calculated based on stator resistance  $R_s$ , signal, actual stator current vector  $I_s$ , actual stator flux amplitude  $\Phi_s$  and position  $\alpha$  as: The  $\alpha$  axes components of the stator reference voltage  $V_{sref}$ , are calculated according to the following equation[5,13]:

$$V_{sref} = \frac{\Phi_{sref} \cos(\alpha_s + \Delta\alpha) - \Phi_{sref} \cos(\alpha_s)}{T_s} + R_s I_{sr} \quad (5)$$

$$V_{sref} = \frac{\Phi_{sref} \sin(\alpha_s + \Delta\alpha) - \Phi_{sref} \sin(\alpha_s)}{T_s} + R_s I_{ss} \quad (6)$$

$$V_{sref} = \sqrt{V_{sref}^2 + V_{sref}^2} \quad (7)$$

$$\alpha_{sref} = \arctan \left( \frac{V_{sref}}{V_{sref}} \right) \quad (8)$$

Where,  $T_s$  is sampling time.

## 3. Voltage Space Vector Modulation.

In the space vector modulation techniques, the reference voltages are given by space voltage vector and the output voltages of the inverter are considered as space vectors. There are eight possible output voltage vectors, six active vectors  $V_1 - V_6$ , and two zero vectors  $V_0, V_7$  (Figure 2). The reference voltage vector is realized by the sequential switching of active and zero vectors. In the Figure.3 there are shown reference voltage vector  $V_{ref}$  and eight voltage vectors, which correspond to the possible states of inverter. The six active vectors divide a plane for the six sectors 1- 6. In the each sector the reference voltage vector  $V_{ref}$  is obtained by switching on, for a proper time, two adjacent vectors

Presented in Figure.1 the reference vector  $V_{ref}$  can be implemented by the switching vectors of  $V_1, V_2$  and zero vectors  $V_0, V_7$

The figure shows the case when the reference vector is in the sector 1.

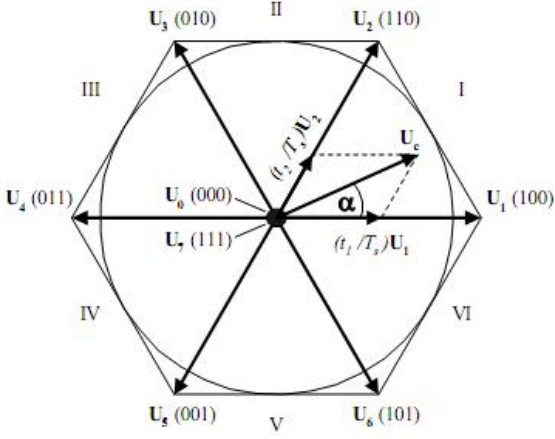


Fig. 3. Principle of the space vector modulation

For example, in the first sector, Vsref is a synthesized voltage space vector and expressed by:

$$V_{sref} = V_0 T_0 + V_1 T_1 + V_2 T_2 \quad (9)$$

The times  $T_1$  and  $T_2$  are obtained by simple trigonometrical relationships and can be expressed in the following equations

$$T_s = T_0 + T_1 + T_2 \quad (10)$$

Where  $T_0$ ,  $T_1$  and  $T_2$  is the work time of basic space voltage vectors  $V_0$ ,  $V_1$  and  $V_2$  respectively. [5-7] [9] The determination of the amount of times  $T_1$  and  $T_2$  is given by simple projections

$$T_1 = \frac{T_s}{2E} \left( \sqrt{6} V_{sref} - \sqrt{2} V_{sref} \right) \quad (11)$$

$$T_2 = \sqrt{2} \frac{T_s}{E} V_{sref} \quad (12)$$

The rest of the period spent in applying the null-vector. For every sector, commutation duration is calculated. The amount of times of vector application can all be related to the following variables:

$$X = \frac{T_s}{E} \sqrt{2} V_{sref} \quad (13)$$

$$Y = \frac{T_s}{E} \left( \frac{\sqrt{2}}{2} V_{sref} + \frac{\sqrt{6}}{2} V_{sref} \right) \quad (14)$$

$$Y = \frac{T_s}{E} \left( \frac{\sqrt{2}}{2} V_{sref} + \frac{\sqrt{6}}{2} V_{sref} \right) \quad (15)$$

The application durations of the sector boundary vectors are tabulated as follows:

Table 1. Durations of the sector boundary vectors.

| SECTOR | 1 | 2  | 3  | 4  | 5  | 6  |
|--------|---|----|----|----|----|----|
| $T_1$  | z | Y  | -z | -x | x  | -Y |
| $T_2$  | Y | -x | x  | z  | -Y | -z |

The goal of this step is to compute the three necessary duty cycles as;

$$T_{aon} = \frac{T_s - T_1 - T_2}{2} \quad (16)$$

$$T_{bon} = T_{aon} + T_1 \quad (17)$$

$$T_{con} = T_{bon} + T_2 \quad (18)$$

The last step is to assign the right duty cycle ( $T_{aon}$ ) to the right motor phase according to the sector.

Table 2. Assigned duty cycles to the PWM outputs.

| SECTOR | 1         | 2         | 3         | 4         | 5         | 6         |
|--------|-----------|-----------|-----------|-----------|-----------|-----------|
| S      | $T_{bon}$ | $T_{aon}$ | $T_{aon}$ | $T_{con}$ | $T_{bon}$ | $T_{con}$ |
| S      | $T_{aon}$ | $T_{con}$ | $T_{bon}$ | $T_{bon}$ | $T_{con}$ | $T_{aon}$ |
| S      | $T_{con}$ | $T_{bon}$ | $T_{con}$ | $T_{aon}$ | $T_{aon}$ | $T_{bon}$ |

#### 4. EKF state estimation.

The Kalman filter is in principle a state observer that gives an estimation of the state variables of a system, by the minimization a square error, when both the system inputs and outputs are subject to random disturbances. The EKF can also be used for unknown parameter estimation [8]. Nonlinear discrete systems model with white noise is given as follows [5] [10,11]:

$$\begin{cases} X(k+1) = f(X(k), u(k)) + W(k) = A_d X(k) + B_d U(k) + W(k) \\ Y(k) = h(X(k)) + V(k) = C_d X(k) + V(k) \end{cases} \quad (19)$$

With:  $w(k)$  is the measurement noise and  $v(k)$ : is the process noise,  $A_d$ ,  $B_d$  and  $C_d$  matrix of discrete system.

$$\begin{cases} A_d = e^{AT_s} \approx I - AT_s \\ B_d = \int_0^{T_s} e^{A(T_s-t)} B dt \approx BT_s \\ C_d = C \end{cases} \quad (20)$$

I: identity matrix of system depending on the size of the state vector[5,6].

Where:,  $U = [V_d \ V_q]^T$  and  $Y = [i_d \ i_q]^T$

$$f_1 = (1 - a_1 R_s(k)) I_d(k) + a_2 \hat{S}_r(k) I_q(k) + a_3 U_d(k)$$

$$f_2 = a_4 \hat{S}_r(k) I_d(k) + (1 - a_5 R_s(k)) I_q(k) + a_7 U_q(k)$$

$$f_3 = a_8 I_d(k) I_q(k) + (1 - a_{10}) \hat{S}_r(k) + a_{11} T_1(k)$$

$$f_4 = a_{12} \hat{S}_r(k) + u(k)$$

$$f_5 = T_1(k) \quad f_6 = R_s(k)$$

$$A_d = \begin{bmatrix} (1 - a_1 R_s(k)) & a_2 \hat{S}_r(k) & 0 & 0 & 0 & a_1 \\ -a_4 \hat{S}_r(k) & (1 - a_5 R_s(k)) & a_6 & 0 & 0 & a_1 \\ a_8 I_q(k) & a_9 & 1 - a_{10} & 0 & a_{11} & 0 \\ 0 & 0 & a_{12} & 1 & 0 & 0 \\ 0 & 0 & 0 & 0 & 1 & 0 \\ 0 & 0 & 0 & 0 & 0 & 1 \end{bmatrix} \quad (21)$$

$$B_d = \begin{bmatrix} a_3 & 0 & 0 & 0 & 0 & 0 \\ 0 & a_7 & 0 & 0 & 0 & 0 \end{bmatrix}^T$$

$$C_d = \begin{bmatrix} 1 & 0 & 0 & 0 & 0 & 0 \\ 0 & 1 & 0 & 0 & 0 & 0 \end{bmatrix}^T$$

$$a_1 = \frac{R_s}{L_d} T_s ; a_2 = \frac{L_q}{L_d} T_s ; a_3 = \frac{1}{L_d} T_s$$

$$a_4 = \frac{L_d}{L_q} T_s ; a_5 = \frac{R_s}{L_q} T_s ; a_7 = \frac{1}{L_q} T_s$$

$$a_8 = p \frac{L_d - L_q}{J} T_s ; a_{10} = \frac{B}{J} T_s ;$$

$$a_{11} = \frac{1}{J} T_s ; a_{12} = p T_s$$

Where:  $f(x(k), u(k))$ : Nonlinear function vector of the states.  $x(k)$ : extended state vector.  $A_d$ : system matrix.  $u_e(k)$  is the control input vector,  $B_d$ : input matrix.  $h(x(k), v(k))$ : Function vector of the outputs.  $C_d$ : Measurement matrix.  $w(k)$  and  $v(k)$ : process and measurement noise respectively. [5] [10,11]

## 5. Application of the Extended Kalman Filter Algorithm.

The extended kalman filter algorithm should be calculated by using matlab-simulink.

### 5.1 Estimation of Error Covariance Matrix.

The prediction covariance is updated by:

$$P(k+1/k) = F(k)P(k/k)F^T(k) + Q(k) \quad (22)$$

Where:  $Q$ : covariance matrix of the system noise,

$$F(k) = \left. \frac{\partial f}{\partial X} \right|_{X(k) = \hat{X}(k/k)} \quad (23)$$

## 5.2 Computation of Kalman Filter Gain.

The Kalman gain is given by (24);

$$L(k+1) = P(k+1/k)C^T(k) \left( C(k)P(k+1/k)C^T(k) + R(k) \right)^{-1}$$

$$\text{Where: } C(k) = \left. \frac{\partial c(x(k))}{\partial x(k)} \right|_{X(k) = \hat{X}(k)} \quad (24)$$

## 5.3 State Estimation.

The extended Kalman correction equation is described by (25).

$$\hat{X}(k+1/k+1) = \hat{X}(k+1/k) + L(k+1)(y(k+1) - C\hat{X}(k+1/k)) \quad (25)$$

## 6. Proposed Sensorless RSM Drive.

The proposed sensorless RSM drive is depicted in Figure 5. The stator flux is estimated by the EKF and used in the DTC control the parameters are listed in Table 3

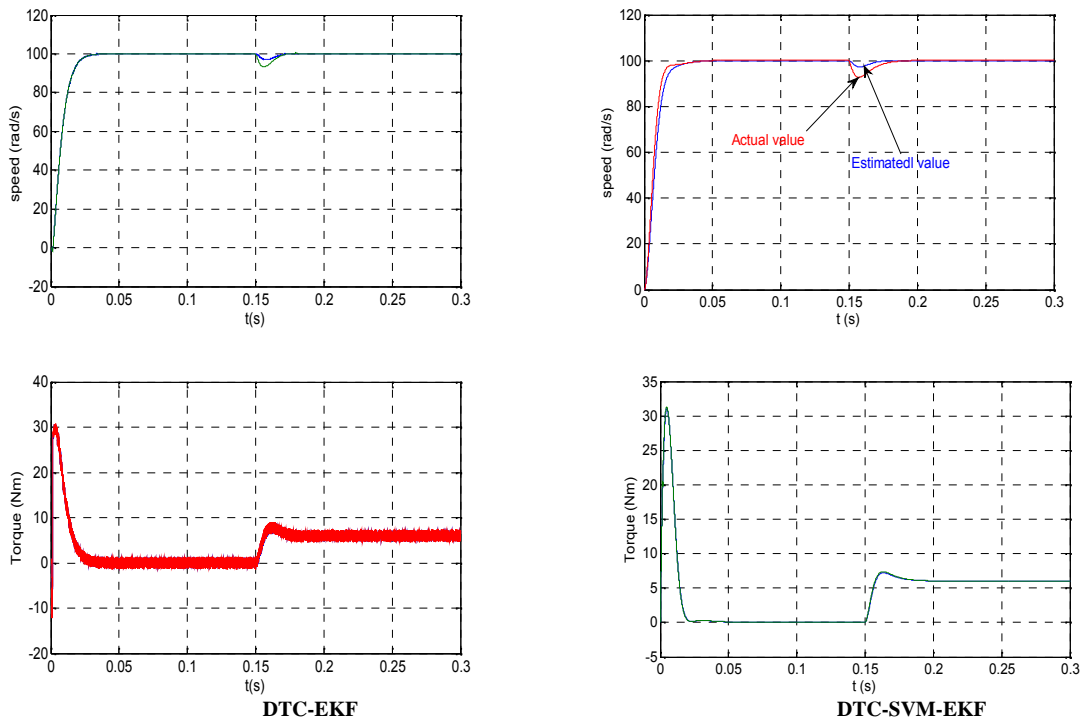
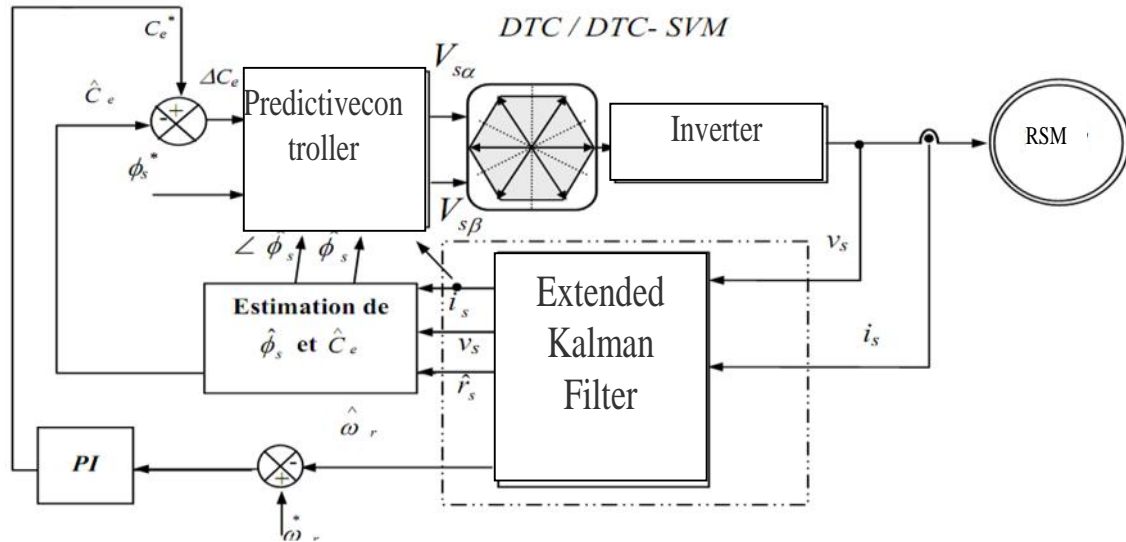
**Table 3.** Durations of the sector boundary vectors.

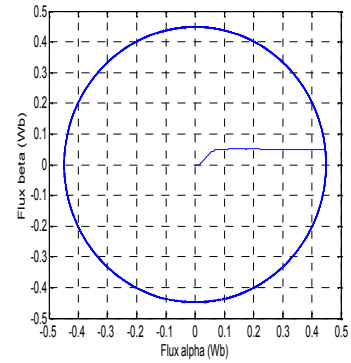
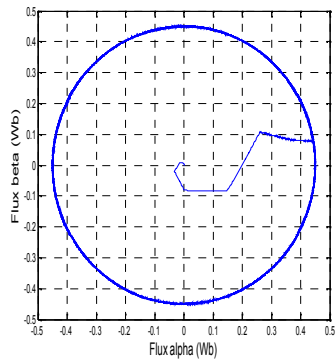
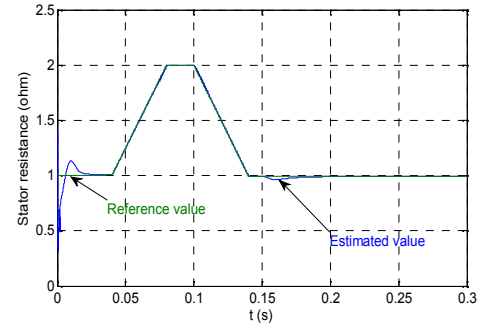
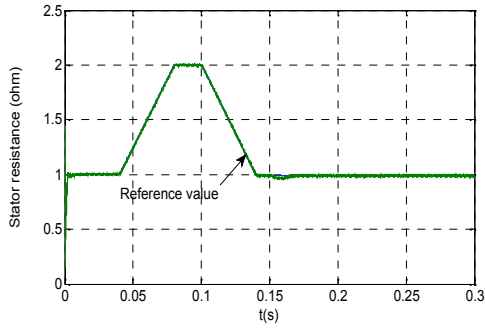
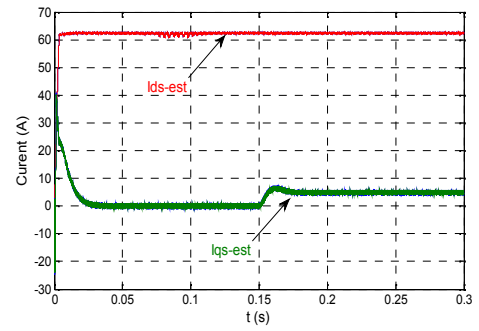
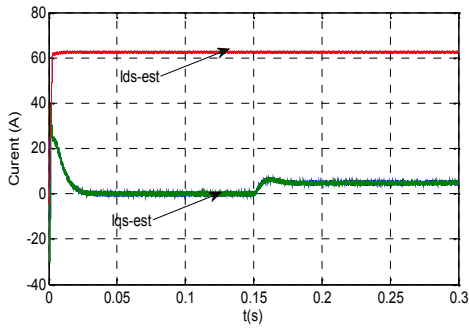
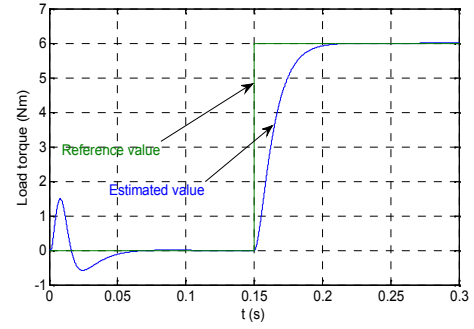
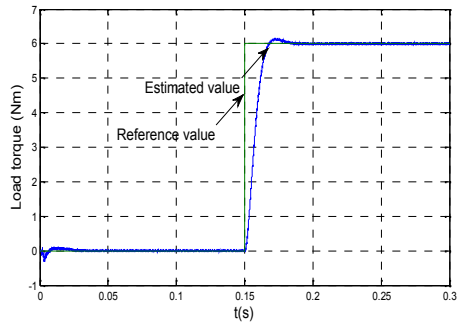
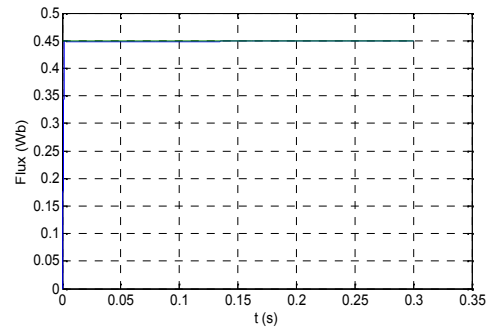
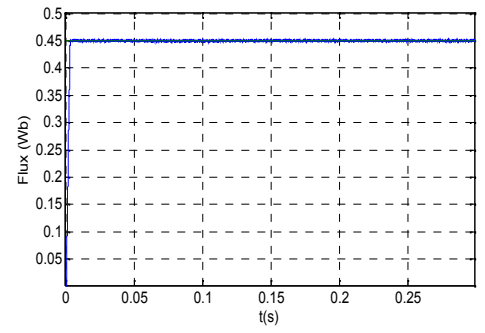
| Parameters of the RSM        |                               |
|------------------------------|-------------------------------|
| Rated torque                 | $T_L = 6 \text{ Nm}$          |
| d-Axis inductance            | $L_d = 0.0072 \text{ H}$      |
| q-Axis inductance            | $L_q = 0.0028 \text{ H}$      |
| Stator resistance            | $R_s = 1$                     |
| Moment of rotor inertia      | $J = 0.003 \text{ kg.m}^2$    |
| Viscous friction coefficient | $F = 0.000035 \text{ Kg.m}^2$ |
| Numbers of pole pairs        | $P = 3$                       |

## 7. Sensorless Drive Simulation Results.

In this section, the effectiveness of the proposed algorithm is verified by computer simulations. During the simulations, the torque set value is limited to 6 N.m (rated torque). In order to show the performances and the robustness of the combined DTC-SVM-EKF algorithm, a series of tests were conducted to check the performance of the proposed DTC-SVM. In all sketched figures, the time axis is scaled in seconds. The block scheme of the investigated direct torque control with space vector modulation (DTC-SVM) for a voltage source inverter fed RSM is presented in (Figure 5). The specifications for the used RSM are listed in table (3).. Figure 6 shows the actual and

DTC-SVM has a significantly lower ripple level both in torque, flux and stator current, a lower current ripple advantageous because the machine will have less EMI noise. Figure 6 show the trajectory of the estimated stator flux components DTC-SVM has as good dynamic response as the classical DTC





**DTC-EKF**

**Classical DTC-EKF**

Fig. 6. Simulation results: A load torque of 6 N.m) is applied at  $t = 0.15$  sec.

## 8. Conclusion.

As an estimator, the Extended Kalman filtering technique is developed for the speed sensorless direct torque control strategy combined with space vector modulation. The complete sensorless solution is presented with the combined DTC-SVM-EKF strategy; low torque ripple operation has been obtained with PMSM. In spite of lower switching frequency, the DTC-SVM scheme has lower harmonic current, and consequently lower ripple than conventional hysteresis based DTC. Simulation results obtained clearly demonstrate the effectiveness of the estimator in estimator in estimating the stator resistance and improving performance of DTC. Additionally, the application of SVM guarantee:

Good dynamic response; High robustness; Low sampling frequency is required; Distortion caused by sector changes is delimited; Inverter switching frequency is constant.

## 9. References.

1. G. Song, Z. Li, Z. Zhao, and X. Wang, . «*Direct Torque Control of Switched Reluctance Motors*», from IEEE Xplore. March 9, 2009.
2. F. Kucuk, H. Goto, H-J. Guo and O. Ichinokura. «*Inductance Vector Angle Based Sensorless Speed Estimation in Switched Reluctance Motor Drive* », The 7th International Conference on Power Electronics, pp 635-639, EXCO, Daegu, Korea October 22-26, 2007.
3. H-J Guo. «*Direct Torque Control of Switched Reluctance Motors*», IEEE ISIE 2006, p.2321-2325 Montreal, Quebec, Canada, July 9-12, 2006.
4. L. Zhong, M. F. Rahman, W.Y. Hu, K. W. Lim, M. A. Rahman. «*A Direct Torque Controller for Permanent Magnet Synchronous Motor Drives* .», IEEE Transactions on Energy Conversion, Vol. 14, p. 637-642, September 1999.
5. S. Belkacem, B. Zegueb and F. Naceri «*Robust Non-Linear Direct Torque and Flux Control of Adjustable Speed Sensorless PMSM Drive Based on SVM Using a PI Predictive Controller*» Journal of Engineering Science and Technology Review 3 (1) 168-175 2010
6. Z. Hilmi Bin Ismail, «*Direct torque control of induction motor drives using space vector modulation (DTC-SVM)* », Master of Engineering Faculty of Electrical Engineering Malaysia (November, 2005).
7. M. P. Kazmierkowski, M. Zelechowski, D. Swierczynski, «*Simple DTC- SVM Control Scheme for Induction and PM Synchronous Motor*», XVII International Conference on Electrical Machines, ICEM 2006, Chania (September 2-5, 2006).
8. I. Boldea, L. Janosi, F. Blaabjerg : *A Modified Direct Torque Control (DTC) of Reluctance Synchronous Motor Sensorless Drive*; Electric Machines & Power Systems; Volume 28, Issue 2, 2000.
9. Z. He, C. Xia ; Y. Zhou: «*Rotor Position Estimation for Switched Reluctance Motor Using support Vector Machine*», Control and Automation, 2007. pp 1683 – 1687.
10. M. Barut, S. Bogosyan and M. Gokasan, «*Switching EKF technique for rotor and stator resistance estimation in speed sensorless control of IMs* *Energy Conversion and Management*», Vol. 48, Issue 12, pp. 3120-3134 (December 2007).
11. M. Kosaka and H. Uda, Sensorless IPMSM drive with EKF estimation of speed and rotor position, Journal of low frequency noise, vibration and active control, Vol. 22, No. 4, pp. 59-70 (2004).
12. M. E. Haque and M. F. Rahman, «*Influence of stator resistance variation on direct torque controlled interior permanent magnet synchronous motor drive performance and its compensation*», IEEE Industry Application Society Annual Meeting, Chicago, USA, Vol. 4, pp. 2563-2569 (2001).
13. C. Yongjun, H. Shenghua, W. Shanming, W. Fang, «*Direct Torque Controlled Permanent Magnetic Synchronous Motor System Based on the New Rotor Position Estimation*», Proceedings of the 26th Chinese Control Conference, Zhangjiajie, Hunan, China, (26-31 July 2007).